Free Radical Biology and Medicine 136 (2019) 22–34

Contents lists available at ScienceDirect

Free Radical Biology and Medicine

journal homepage: www.elsevier.com/locate/freeradbiomed

Original article

Mitochondria and oxidative stress in ovarian endometriosis

Chaolu Chen, Yong Zhou, Changchang Hu, Yinfeng Wang, Zhuqing Yan, Zhi Li, Ruijin Wu*

Department of Gynecology, Women's Hospital, School of Medicine, Zhejiang University, Zhejiang, 310006, China

ARTICLE INFO

Keywords:
Ovarian endometriosis
Reactive oxidative species
Mitochondria
Mitochondrial superoxide dismutase
Oxidative stress

ABSTRACT

Endometriosis is associated with inflammatory reaction, and reactive oxidative species (ROS) are highly pro-inflammatory factors. Mitochondria are responsible for the production of ROS and energy. However, little is known about how mitochondria regulate ROS generation and energy metabolism in endometriosis. In our study, we investigated mitochondrial structure and function of ectopic endometrial stromal cells (ESCs) in ovarian endometriosis. We found mitochondria in ectopic ESCs generated more ROS and energy than controlled groups. Mitochondrial superoxide dismutase (SOD2), as an antioxidant enzyme, was found highly expressed in ectopic endometrium compared with normal endometrium. Due to its antioxidant role, SOD2 promoted the development of endometriosis by maintaining functional mitochondria to support high energetic metabolism of ectopic ESCs. We also showed that SOD2 promoted cell proliferation and migration in ovarian endometriosis. Inhibiting SOD2 expression reduced proliferation and migration of ectopic ESCS, and increased cell apoptosis. Therefore, understanding the role of mitochondrial dysfunction and SOD2 in ovarian endometriosis may provide new strategies to treat this disease.

1. Introduction

Endometriosis, as an ectopic location for endometrial tissues outside of the uterine cavity, mostly located in ovarian, is a considerable threat to the physical, psychological, and social integrity of women, causing pelvic pain and infertility in 10–15% women [1–3]. Despite intensive research, its mechanistic rationale still remains elusive. Recent studies have shaped the idea that oxidative stress might be anticipated in the initiation or progression of endometriosis [4–6]. Markers of oxidative stress in peritoneal fluid, follicular fluid, and peripheral circulating blood are significantly elevated in patients with endometriosis [7–10]. When the balance between reactive oxidative species (ROS) generation and detoxification is disrupted, the relative excess of ROS results in oxidative stress. ROS are oxygen-containing reactive chemical species, examples including superoxide (O_2^-), hydroxyl radicals (·OH) and hydrogen peroxide (H_2O_2). High amounts of ROS can damage peritoneal mesothelial cells and promote the ectopic endometrium implantation [11]. Also, it can change the morphology and function of vascular endothelial cells, including permeability and adhesion molecule expression, thus enhancing the adhesion between inflammatory cells and endothelial cells, further leading to persistent inflammation [12,13]. As a second messenger, ROS can activate protein kinase B (AKT) and NF-κB pathway to promote the development of endometriosis [14,15].

ROS are mainly produced by the mitochondrial electron transport chain in the process called oxidative phosphorylation (OXPHOS), mostly by the respiratory chain complex I and complex III. Mitochondria cristae are major site for OXPHOS. The expansion of cristal spaces occurs with activation of OXPHOS and increased ROS generation. It is estimated that mitochondria consume 90% of cellular oxygen and 2% of that oxygen is reduced by electrons to form ROS. Human mitochondrial DNA (mtDNA) encodes 13 subunits of the electron transport chain. MtDNA is more vulnerable to oxidative damage than nuclear DNA, which may alter the replication and transcription of mtDNA, hence affecting the overall mitochondrial function and ROS generation [16]. Recent discoveries have found some mtDNA mutations, which encode subunits of complex I in patients with endometriosis. These mutations will affect the normal electron transport chain, resulting in increased electron leakage and ROS [17,18]. Although we have known mitochondria are major sources for ROS generation in the development of endometriosis, what happens to mitochondria in the patients with endometriosis is less clear. Mitochondrion is also an essential organelle crucial in energy generation, cellular aerobic respiration and apoptosis-programmed cell death except producing ROS. Research on mitochondrial ultrastructure, respiration function and the expression of OXPHOS dependent genes encoded by mtDNA, will help us firstly unveil the relation between mitochondrial change and oxidative stress in ovarian endometriosis.

Mitochondrial superoxide dismutase (SOD2), localized in the

* Corresponding author.
E-mail address: wurj@zju.edu.cn (R. Wu).

https://doi.org/10.1016/j.freeradbiomed.2019.03.027
Received 15 February 2019; Received in revised form 21 March 2019; Accepted 25 March 2019
Available online 27 March 2019

mitochondria, is an antioxidant enzyme, playing a crucial role in maintaining cellular ROS balance. SOD2 catalyzes the dismutation of $O_2^{\cdot-}$, leading to the formation of H_2O_2, which is detoxified by glutathione peroxidases (GPx) or catalase to H_2O and O_2. Optimal protection is achieved only when an appropriate balance among three enzymes is maintained. Some scientists demonstrated that high ratios SOD2/GPx1 led to an accumulation H_2O_2 at least in the mitochondria. Higher levels of H_2O_2 favor proliferation and metastasis in aggressive tumors [19]. Several recent studies found that in women with endometriosis, the eutopic and ectopic endometrium overexpressed enzymes like SOD2 involved in defense against oxidative stress [20–22]. Enhanced ROS production in ectopic lesions may induce SOD2 overexpression as a response to oxidative stress. For this reason, SOD2 was characterized as disease suppressor gene, providing sustainable protection against ROS. However, recent literature suggested that SOD2 had a dichotomous role in ovarian tumor proliferation and metastasis, which means SOD2 not only protected cells from mitochondrial ROS, but also promoted tumor progression [23]. Despite its antioxidant role, to date, little is known about its other functions in endometriosis. Given that some ovarian cancer stem from endometriosis, in this study, we observed the role of SOD2 in mitochondrial function and how SOD2 functions besides its antioxidant role in ovarian endometriosis.

2. Materials and methods

2.1. Patients and samples collection

This study was approved by the Ethics Committee of Women's Hospital, School of Medicine, Zhejiang University. All women provided informed written consent before being recruited. We collected endometrial tissues from inpatients of Women's Hospital, Zhejiang University from June 2017 to January 2019. The subjects consisted of 113 women who had regular and biphasic menstrual cycle. We obtained endometrial tissues from 35 childbearing age women (mean age: 33.9 ± 6.8 years old) undergoing hysteroscopy for other benign gynecological diseases without endometriosis as control group (CE). The ectopic endometrial tissues were obtained from ovarian endometriotic lesions (EC, n = 78, mean age: 33.0 ± 6.5 years old), and their homologous eutopic endometrium (EU, n = 38, mean age: 34.6 ± 6.2 years old) from the same women diagnosed with stage III–IV endometriosis (according to revised AFS classification) who had undergone laparoscopy and hysteroscopy. All specimens were in the proliferative phase of the cycle, which was confirmed by histological examination and basal body temperature monitoring. After surgical remove, some tissues were fixed in 10% paraformaldehyde and embedded in paraffin for immunohistochemistry studies, others were transferred to the DMEM/F12 medium under sterile conditions and transported to the laboratory on ice for cell culture. The details of sample grouping in this study were shown in study flowchart (Fig. 1).

All the enrolled women had regular menstruation and were free of hormonal medications for at least 6 months. We excluded anyone with diabetes mellitus, hypertension, autoimmune disorder, neoplastic and severe medical diseases from this study. Patient demographic and baseline characteristics in age, parity and BMI were not statistically significant among three groups.

2.2. Isolation and culture of endometrial stromal cells

The tissues were washed with phosphate-buffered saline (PBS) and then cut into pieces. These pieces were digested with type I collagenase (0.2%, Sigma, USA) for 1 h at 37 °C in the constant temperature shaker. After removing debris and epithelial cells by 100 μm and 40 μm cell strainer respectively, endometrial stromal cells (ESCs) were resuspended in DMEM/F12 containing 10% fetal bovine serum (FBS) and incubated in 5% CO2 at 37 °C. The purity of ESCs was confirmed by immunohistochemistry using Vimentin and Cytokeratin 7 respectively as markers of stromal and epithelial cells. The number of Vimentin positively stained cells was above 95% in our study (Fig. 2A B). The cell viability was checked above 90% before cellular experiments.

2.3. Mitochondrial superoxide measurement by flow cytometry

As an indicator of mitochondrial superoxide, MitoSox Red dye (Invitrogen, M36008) were monitored by live cell imaging according to manufacturer's instructions. The endometrial stromal cells were plated in 6-well plates at a density of 3×10^5 per well. The plate was incubated at 37 °C with 5% CO_2. At the following day, we digested the adherent endometrial stromal cells using trypsin, then centrifuged at 1000 rpm for 5min and the supernatant was discarded. After washing cells with PBS, the treated cells were applied with 200 μL 5 μM MitoSox working solution at 37 °C for at 30 min. We prepared the MitoSox working solution according to the instructions. Then we washed cells gently three times with PBS and resuspended cells with PBS for detecting oxidation by flow cytometry, the measurements were carried out using Cytoflex (Beckman, USA). MitoSox Red was excited by laser at 510 nm, and emitted by laser at 580 nm. Each sample was set with triplicate wells in one experiment and we also prepared a group with PBS and Mitosox to alleviate the impact of PBS on measurements. The data presented by fold change of mean fluorescent intensity of MitoSox fluorescence when compared with PBS negative control.

2.4. Transmission electron microscopy

Transmission electron microscopy was performed as previously described [24]. To visualize the ultrastructural morphology of mitochondria, we digested 4×10^6 endometrial stromal cells using trypsin, then centrifuged at 1000 rpm for 5min and the supernatant was discarded. After washing cells with PBS, the treated cells were fixed with 2.5% glutaraldehyde at 4 °C for at least 4 h and then fixed with 1% osmic acid at room temperature for 1 h. Following this, the samples were routinely prepared through dehydrating gradiently with 50%, 70%, 90%, 100% ethanol solution and 100% acetone solution for 15 min respectively in room temperature, embedding for 4 h at room temperature and cutting into 70 nm ultrathin sections by microtome, then the sections were placed on copper grids and stained with uranyl acetate and lead citrate for evaluation. They were observed under a transmission electron microscope (FEI Tecnai T10, USA) at a magnification of 4800 × for examining mitochondrial distribution and quantity in cells, at 49,000 × and 98,000 × for examining mitochondrial structure. For morphometric analysis of mitochondria in sections, each section was randomly observed for five different fields. We observed mitochondria quantity, array of cristal and measured mitochondrial length in three groups by Image-Pro Plus 6.0 software and assigned mitochondria to morphological classes I-III [25].

2.5. Seahorse XF96 extracellular flux analysis

The oxygen consumption rate (OCR) and extracellular acidification rate (ECAR) were measured using the Seahorse XF96 Extracellular Flux Analyzer (Seahorse Bioscience), as described elsewhere [26–28]. The endometrial stromal cells were plated in Seahorse 96-well microplates at a density of 30,000 per well. The plate was incubated at 37 °C with 5% CO_2. Each sample was set with sextuplicate wells. At the following day 1 h prior to the assay, the media was replaced with XF medium. OCR was measured at baseline and after injection of the mitochondrial stress test kit: oligomycin (1 μmol/L; complex V inhibitor, inhibits ATP synthase), FCCP (1 μmol/L; OXPHOS uncoupler), and rotenone/antimycin A (1 μmol/L, 5 μmol/L; complex I and III inhibitor, respectively). Maximal respiration was normalized by subtracting non-mitochondrial respiration (after antimycin A & rotenone addition). ATP-linked OCR was derived as oligomycin–inhibited OCR. The FCCP-stimulated OCR was defined as the difference between maximal respiration and basal

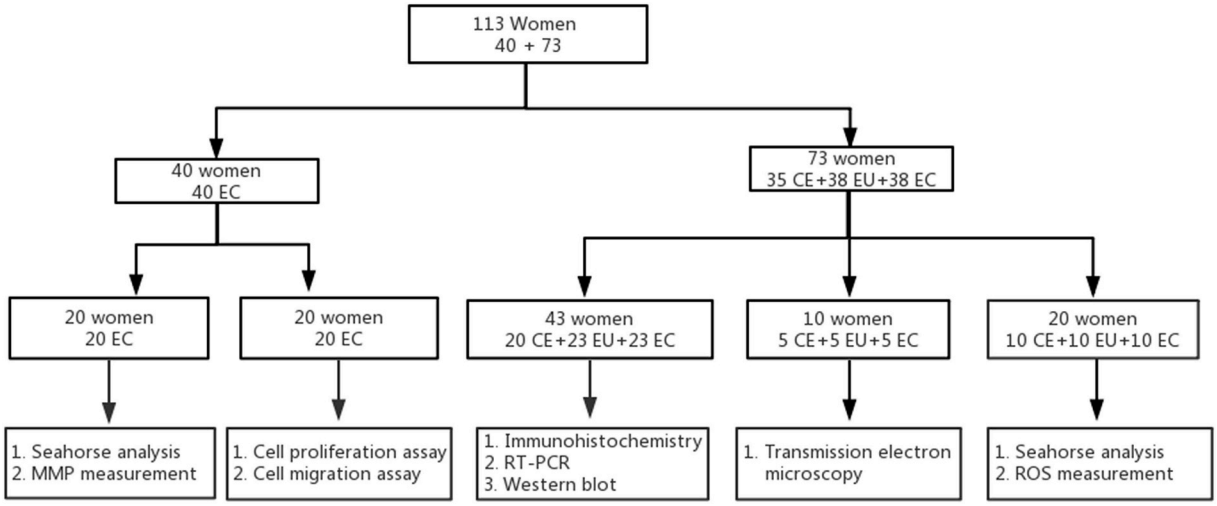

Fig. 1. Flowchart of sample grouping for different experiments.

respiration, which can be used to evaluate spare respiratory capacity. ECAR were also taken at baseline and after injection of the glycolysis stress test kit: glucose (10 mmol/L), oligomycin (1 μmol/L) and 2-DG (50 mmol/L, glucose analog). Sequential compound injections measured glycolysis, glycolytic capacity and allowed calculation of glycolytic reserve and non-glycolytic acidification.

Despite the strong correlation of ECAR with glycolytic activity, other sources of acidification (mainly mitochondrial-derived CO_2 [29–31]) can limit the specificity of the measurement. We used the Glycolytic Rate Assay kit to determine the total proton efflux rate (PER) as a result of bulk acidification and the glycolytic proton efflux rate (glycoPER) correlated with lactate accumulation, an accurate measurement of basal glycolysis. Basal rates of OCR and ECAR were measured first, then rotenone & antimycin A (0.5 μM final concentration) were injected to measure the amount of OCR caused by mitochondrial activity, which is used to determine and subtract mitochondrial contribution to acidification. The injection of 2-DG (50 mM final concentration) provided data about glycolysis. The data shown was from three independent experiments and was generated using Seahorse Report Generator software. To allow comparison among three groups, data were normalized to total cell protein in individual wells determined by the Bradford protein assay (Bio-Rad).

2.6. Immunohistochemistry

The expression of SOD2 was examined by immunohistochemical detecting procedures [32]. In brief, tissues were cut into 5-μm sections. Following deparaffinized and dehydrated, antigen retrieval was performed by heating in microwave oven for 10 min. Incubation with 3% hydrogen peroxide for 30 min was to quench the endogenous peroxidase activity after cooling to room temperature and rinsing in PBS. Primary antibody against SOD2 (1:100, ab68155, Abcam) was performed for 1 h, then they were incubated with secondary antibody (DAKO, Denmark) for 30 min at room temperature. After stained by diaminobenzidine (DAKO, Denmark) for 5 min, they were observed under a microscope (Leica LMD, Germany). Negative controls for immunostaining were performed by replacing the primary antibodies with the appropriate non-immune IgG isotypes. A section of fallopian tube with high SOD2 expression was set as positive control. Sections would be recorded as positive if it colored brown. A semi-quantitative analysis was carried out with the Image-Pro Plus 6.0 software to measure the staining intensity of sections. The integrated optical density (IOD)of the brown part, divided by the total area, obtained mean optical density (MOD). MOD was proportional to the expression of the corresponding protein. Each section was measured in five different fields.

2.7. Reverse transcription and quantitative real-time PCR (RT-qPCR)

Total RNA was extracted from ESCs using the RNAiso Plus reagent (Takara Bio, Japan) according to the manufacturer's instructions. 1 μg of total RNA was reverse transcribed in a 20 μl volume by PrimeScript™ RT reagent Kit with gDNA Eraser (Takara Bio, Japan). Real-time PCR was performed with 7900HT Sequence Detection System (Applied Biosystems, Foster City, CA) using SYBR Premix Ex Taq™ kit (Takara Bio, Japan). The amplification includes 40 PCR cycles of 95 °C for 30 s, 95 °C for 5 s and 60 °C for 30 s. Specific primers used for PCR amplification were synthesized by Sangon (Shanghai, China) with the following sequences: GAPDH (a housekeeping gene).

5′-TCAGTGGTGGACCTGAC-3′ (forward) and
5′-TGCTGTAGCCAAATTCGTT-3′ (reverse); ND1
5′-ACTACAACCCTTCGCTGACG-3′(forward) and
5′-CCGATCAGGGCGTAGTTTGA-3′(reverse); ND6
5′-GGGGTTTGTGGGGTTTTCTTC-3′(forward) and
5′-CCCACAGCACCAATCCTACC-3′(reverse); CytB
5′-CCCATCCAACATCTCCGCAT-3′(forward) and
5′-GAGGCGTCTGGTGAGTAGTG-3′(reverse); Cox1
5′-ATACCAAACGCCCCTCTTCG-3′(forward) and
5′-TGTTGAGGTTGCGGTCTGTT-3′(reverse); ATPase 6
5′-TGCCACAACTAACCTCCTCG-3′(forward) and
5′-GGTAAGAAGTGGGCTAGGGC-3′(reverse); ATPase 8
5′-AAACTACCACCTACCTCCCTCA-3′(forward) and
5′-GGCAATGAATGAAGCGAACAGA-3′(reverse); SOD2
5′-GGAAGCCATCAAACGTGACTT-3′ (forward) and
5′-CCCGTTCCTTATTGAAACCAAGC-3′ (reverse); GPx1
5′-CAGTCGGTGTATGCCTTCTCG-3′(forward) and
5′-GAGGGACGCCACATTCTCG-3′(reverse)

We set triplicate wells for each sample to calculate its average cyclic threshold (Ct) value. The relative expression levels of target genes were analyzed using the $2^{-\Delta\Delta Ct}$ method. Relative mtDNA copy number levels were calculated by quantitating mtDNA copy numbers relative to nuclear DNA, as detailed elsewhere [33].

2.8. Protein extraction and western blot analysis

Cells were washed twice in PBS prior to being disintegrated in lysis buffer (RIPA, Beyotime, China) on ice for 30 min and then centrifuged at 14,000 rpm for 15 min at 4 °C. The protein concentrations were quantified by the BCA assay kit (Thermo Scientific, USA). Equal amounts of proteins were isolated electrophoretically in 12% sodium

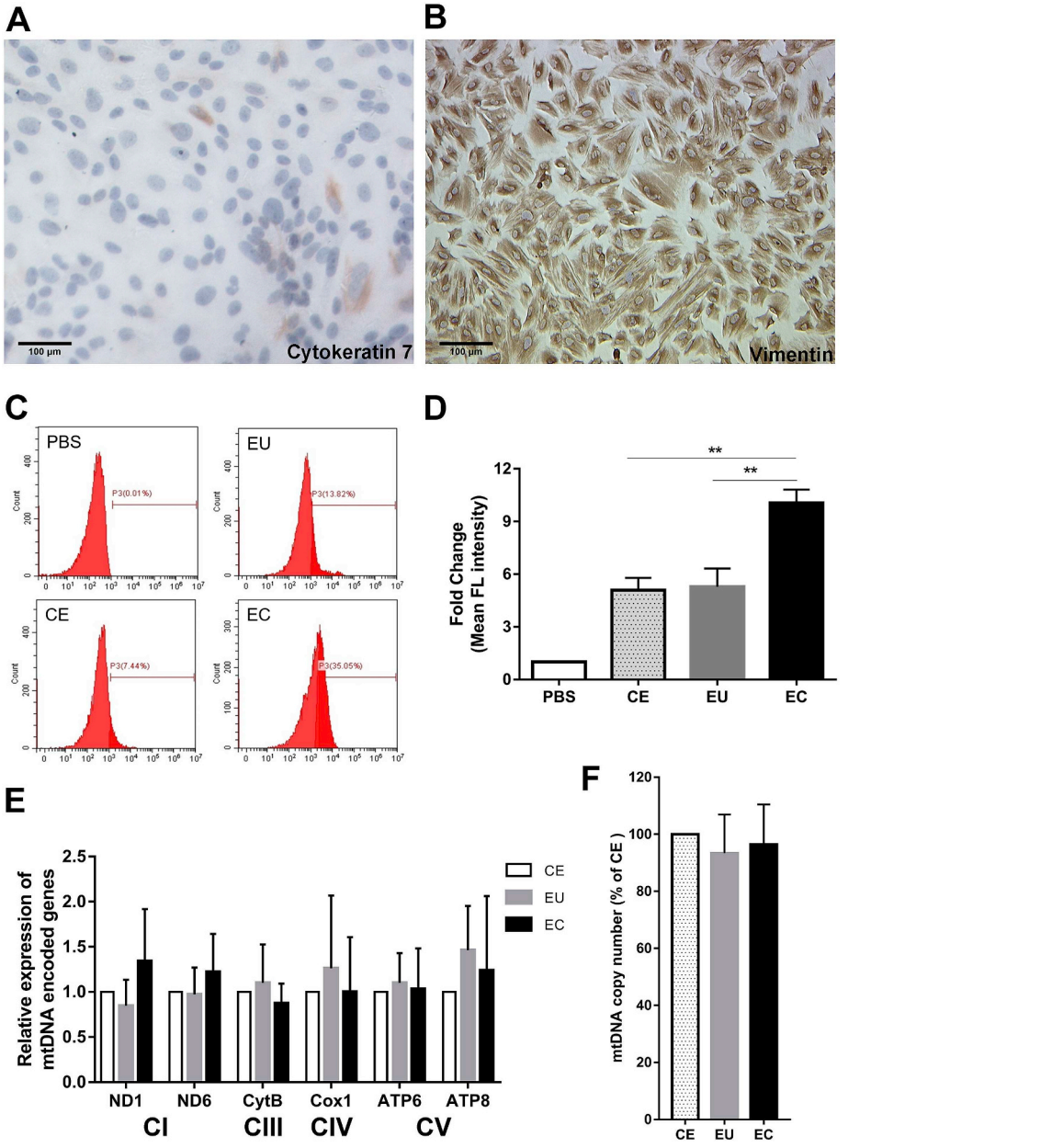

Fig. 2. Mitochondrial superoxide and mtDNA of ectopic (EC), eutopic (EU) and controlled (CE) stromal cells. Identification of primary cultured ESCs (200 ×). A. Negative for Cytokeratin 7. B. Positive for Vimentin. C. Representative histogram of flow cytometry experiments demonstrating increase in mean fluorescent intensity of Mitosox from controlled ESCs to ectopic ESCs as indicated. D. Quantitative data expressing changes in mean fluorescent intensity of Mitosox among three groups. E. Analysis of the mtDNA encoded genes. F. Analysis of mtDNA copy numbers.

dodecyl sulfate polyacrylamide gel (SDS-PAGE) and electrotransferred to polyvinylidene fluoride membranes (Millipore, Billerica, MA, USA). Membranes were blocked in 5% bovine serum albumin (BSA, Sigma-Aldrich, St Louis, MO, USA) at room temperature for 1 h and then incubated with primary rabbit antibodies against SOD2 (1:1000, ab68155, Abcam) and β-Actin (1:4000, ab8227, Abcam) at 4 °C overnight, respectively. The membrane was further incubated with horseradish peroxidase-conjugated goat anti-rabbit secondary antibodies (1:10,000, Abcam) for 1 h at room temperature. The signals were detected by enhanced chemiluminescence detection reagent (Sigma-Aldrich, St Louis, MO, USA). The relative protein levels were quantified normalized to β-Actin expression by Image J software.

2.9. RNA interference by small interfering RNA

RNA interference in ectopic endometrial stromal cells was performed by small interfering RNA (siRNA) transfection. Scramble non-targeting control and SOD2-specific siRNA oligonucleotides were synthesized by GenePharma Corporation (Shanghai, China) with the following target sequences:

5′-GCAUCUGUUGGUGUCCAAGTT-3′(sense) and
5′-CUUGGACACCAACAGAUGCTT-3′(antisense)

Ectopic endometrial stromal cells (1×10^5) were seeded in a six-

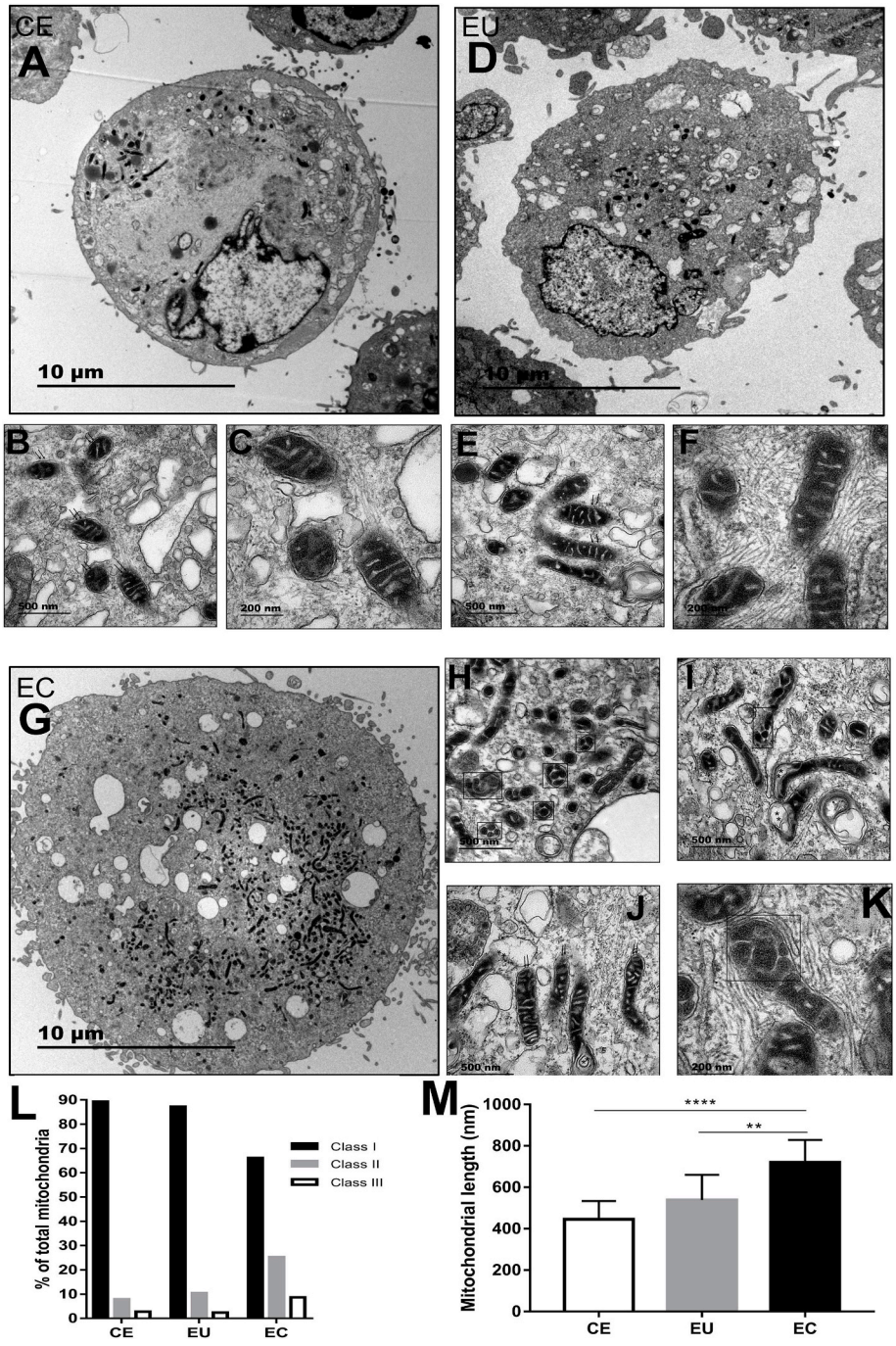

Fig. 3. Representative transmission electron microscopy fields of mitochondria ultrastructure of ectopic (EC), eutopic (EU) and controlled (CE) stromal cells. Double arrow indicate class I mitochondria. Square indicate class II mitochondria. Double asterisk denotes electron-translucent area, representing class III mitochondria. The scale bar = 10 μm, 500 nm, 200 nm. A–C: TEM images of controlled ESCs and structure of mitochondria from controlled ESCs. D–F: TEM images of eutopic ESCs and structure of mitochondria from eutopic ESCs. G–K: TEM images of ectopic ESCs and structure of mitochondria from ectopic ESCs. L. Morphometric analysis of mitochondria. Mitochondria were assigned to morphological class I–III. M. Average mitochondrial major axis length. Data represent three independent experiments (five mitochondria/cell, at least 25 cells/experiment). The ectopic ESCs had longer mitochondrial than eutopic ESCs (**P < 0.01) and controlled ESCs (****P < 0.0001).

well culture plate 1 day before transfection. Control siRNA or SOD2-specific siRNA were transfected into the cells using 30 nM Lipofectamine RNAiMAX (Invitrogen). Cells were lysed for RT-qPCR after 48 h transfection and for western blot after 72 h. The experimental transfection efficiencies ranged from 80 to 90%.

2.10. Cell proliferation assay

Ectopic endometrial stromal cells were seeded at a density of 5×10^3 per well in 100 μl culture medium in four 96-well culture plates, transfected by SOD2 siRNA or control siRNA for 0, 24, 48 and 72 h after the adherent cells growth. The cells were incubated with 10 μl/well cell Counting Kit-8 (DOJINDO, CK04-13) solutions for 3 h at 37 °C, protected from light. The optical density (OD) in the medium was examined at 450 nm using a micro plate reader.

2.11. Cell migration assay

The ESCs migration assay was carried out in transwell chambers with 6.5 mm diameter and 8 μm pore size filter (Corning, NY, USA) inserts for 24-well culture plates. Ectopic stromal cells were transfected by SOD2 siRNA or control siRNA for 12 h, and after transfection, cells were detached and resuspended with a density of 5×10^4 in 200 μl DMEM/F12 without serum before seeded on the upper chamber. The lower chamber was filled with 500 μl DMEM/F12 containing 10% FBS. After 24 h, cells were fixed on the bottom of the membrane and then dyed with crystal violet solution. The cells were photographed and counted under a light microscope (100 × ,200 ×). Each chamber was randomly counted for five fields and migration assays were repeated in triplicate.

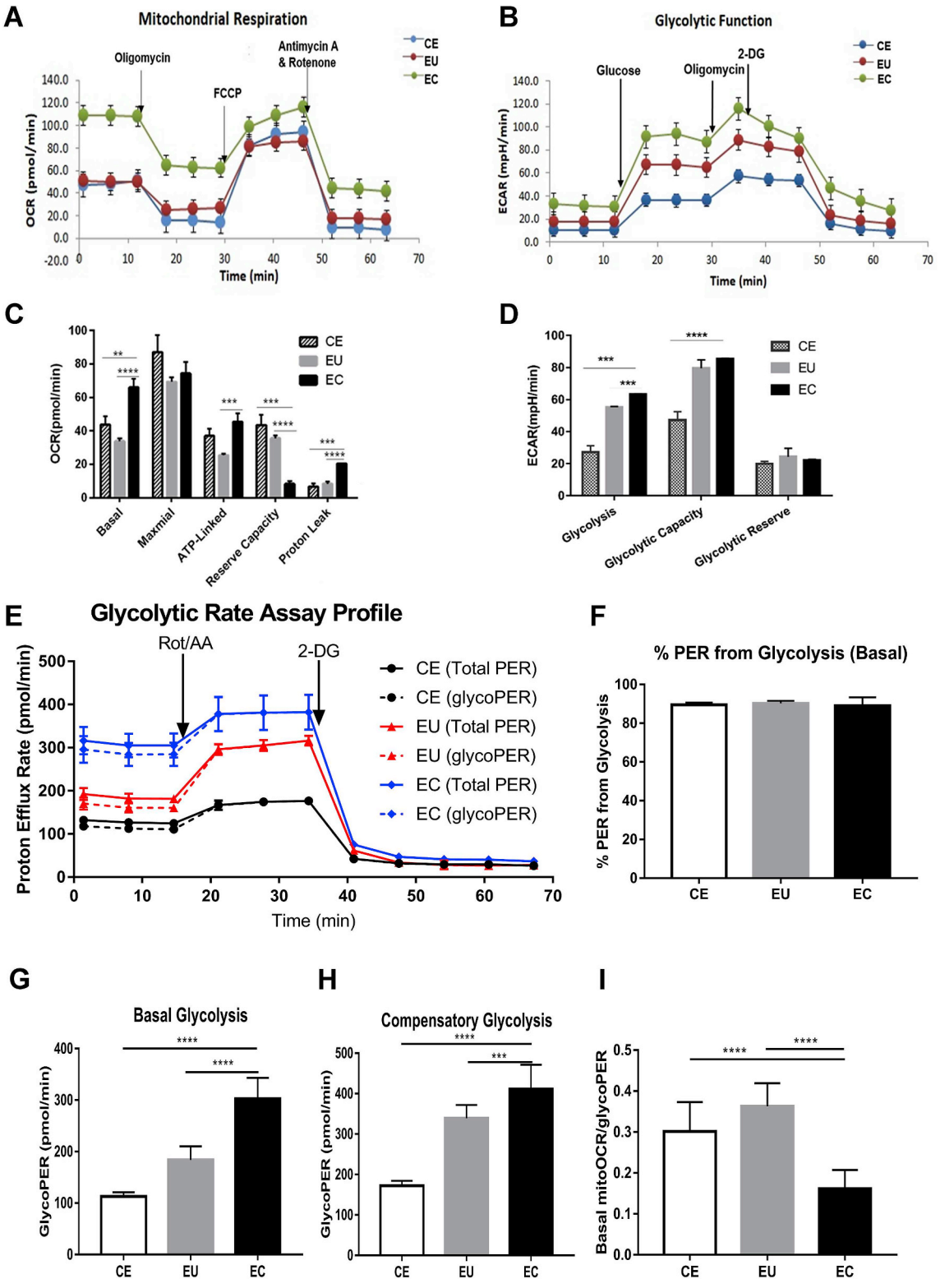

Fig. 4. Mitochondrial respiration of ectopic (EC), eutopic (EU) and controlled (CE) stromal cells. A. OCR was measured using extracellular flux analysis. Oligomycin was used to derive ATP-linked OCR, FCCP to stimulate maximal OCR, and antimycin A and rotenone to inhibit all mitochondrial OCR. B. ECAR was measured to represent glycolytic function including glycolysis, glycolytic capacity and glycolytic reserve. C. Mitochondrial respiration of ectoic ESCs were more energetic than eutopic and controlled ESCs. D. Glycolytic function of ectopic ESCs were significantly higher than eutopic and controlled ESCs. E. Representative of glycolytic rate assay profile. F. The %PER from glycolysis of three groups. G-I. Quantitative data of basal glycolysis, compensatory glycolysis and basal mitoOCR/glycoPER ratio in three groups.

2.12. Mitochondrial membrane potential (MMP, ΔΨm)

Changes in cellular MMP were determined using JC-10 mitochondrial membrane potential staining kit (MAK160, Sigma, USA). The ectopic ESCs were seeded at a density of 3×10^5 cells in 6-well culture plates. After the adherent cells growth, they were transfected by SOD2 siRNA or control siRNA for 12 h at 37 °C in a CO2 incubator. In parallel, we incubated ectopic ESCs with 5 μM FCCP for 30min as positive control samples. FCCP treatment for ectopic ESCs was sufficient to induce apoptosis in cells, which was titrated before the assay. We prepare the JC-10 dye loading solution by adding 25 μl of the 200 × JC-10 to 5 ml of assay buffer. Then adherent cells were detached with trypsin, collected by centrifugation, resuspended in 500 μl of the JC-10 dye loading solution and incubated at 37 °C in a 5% CO_2 incubator for 30 min, protected from light. The stained cells were then collected by centrifugation and washed with assay buffer. After washing, the cell suspension was centrifuged once more and then resuspended in 1 mL assay buffer. Fluorescence intensity was evaluated using a flow cytometer (Cytoflex, Beckman, USA) in the FL1 (green) and FL2 (red) channnels. When the MMP is high, JC-10 is concentrated in the matrix of mitochondria, forming J-aggregates, generating red fluorescence. In apoptosis cells, MMP collapse results in the failure to retain JC-10 in the mitochondria, therefore JC-10 becomes monomer, producing green fluorescent. The kit was used to determine the loss of MMP in cells. The relative ratio of red-green fluorescence was used to represent MMP.

2.13. Statistical analysis

Data were presented as means ± SD at least three independent experiments. Student's t-test was used to analyze differences for paired data and one-way ANOVA was used to analyze multiple comparisons. A value of $P < 0.05$ was considered as statistically significant.

3. Results

3.1. Mitochondrial superoxide and mitochondrial DNA of endometrial stromal cells

To investigate differences of mitochondrial superoxide among controlled endometrial stromal cells (CE), eutopic endometrial stromal cells (EU) and ectopic endometrial stromal cells (EC), we used the mitochondria-targeted redox-sensitive dye Mitosox. As shown in Fig. 2C, enhanced fluorescence intensity of Mitosox were found in ectopic ESCs. The production of mitochondrial superoxide in ectopic ESCs was increased by 90% and 98% compared with eutopic ESCs and controlled ESCs respectively (Fig. 2D, $P < 0.01$). Results were normalized to fluorescence intensity of PBS. We also used PCR to examine six mtDNA encoded electron transport chain subunits including ND1, ND6 (in complex I), cytochrome b (in complex III), Cox1 (in complex IV) and ATPase 6, ATPase 8 (in complex V) in three groups. As shown in Fig. 2E and F, no significant difference was found in mtDNA copy numbers and transcription among CE, EU and EC groups. The disease did not lead to any changes of these complex subunits in transcription level.

3.2. Mitochondrial ultrastructure of endometrial stromal cells

To assess mitochondrial ultrastructure of endometrial stromal cells, we used transmission electron microscope (TEM) at a magnification of 4800×, 49000× and 98000×. In ESCs, mitochondria were located closely to the plasma membrane or in the vicinity of the nuclear (Fig. 3A, D and G). In controlled (Fig. 3B and C) and eutopic ESCs (Fig. 3E and F), the majority of mitochondria were assigned to class I morphology. They displayed more oval-like, containing intact outer mitochondrial membrane and groups of parallel cristae. The cristae extended across the whole body of the organelle with apparent and narrow intracristal spaces. In ectopic ESCs (Fig. 3H and K), there seemed to be more mitochondria, and they appeared longer than those of controlled and eutopic ESCs, with over 60% class I mitochondria exhibiting increased amount of cristae and electron density of matrix. Some mitochondria of ectopic ESCs were noted as class II, characterized by distinctive morphological appearance of cristae. The cristae were no longer organized in parallel, instead looking like circular structures disconnected from outer membrane. Only a few mitochondria of ectopic ESCs were entitled class III, which had asymmetric swollen electron-translucent areas devoid of cristae in one side of the mitochondria. We also performed morphometric analysis on mitochondria (Fig. 3L, M). The results showed class I mitochondria predominated in three groups and the ectopic ESCs had more class II-III mitochondria than those of CE and EU groups. Also, mitochondria were elongated in ectopic ESCs than those of CE and EU groups.

3.3. Mitochondrial respiration of endometrial stromal cells

To evaluate mitochondrial respiration and understand cellular metabolic features, we examined the oxygen consumption rates (OCR), representing mitochondrial oxidative phosphorylation and extracellular acidification rate (ECAR), correlating with glycolytic activity using extracellular flux analysis in controlled, eutopic and ectopic ESCs (Fig. 4A and B). As shown in Fig. 4C, the basal OCR in ectopic ESCs was 95% higher than eutopic ESCs ($P < 0.0001$) and 51% higher than controlled ESCs ($P < 0.01$). ATP-linked OCR in ectopic ESCs was 79% higher than eutopic ESCs ($P < 0.001$). Reserve capacity in ectopic ESCs was 77% lower than eutopic ESCs ($P < 0.0001$) and 81% lower than controlled ESCs ($P < 0.001$). As for proton leak, ectopic ESCs was significantly increased than eutopic ESCs and controlled ESCs. The above observations indicated that ectopic ESCs had incremental mitochondrial oxidative phosphorylation for energy needs. As shown in Fig. 4D, glycolysis in ectopic ESCs was 14% higher than eutopic ESCs ($P < 0.001$) and 132% higher than controlled ESCs ($P < 0.001$), glycolytic capacity in ectopic ESCs was 81% higher than controlled ESCs ($P < 0.0001$). No significant difference of glycolytic capacity was found between ectopic ESCs and eutopic ESCs. These results supported that ectopic endometrial stromal cells depended on both oxidative phosphorylation and glycolysis to provide energy for cellular function and activity. Besides, they were significantly more energetic with high levels of mitochondrial oxidative phosphorylation and glycolysis.

Given that ECAR overestimates the true basal glycolysis [29], we further analyzed the metabolic switch using the Glycolysis Rate assay to quantify the PER and the GlycoPER (Fig. 4E). The %PER from glycolysis represents the contribution of the glycolytic pathway to total extracellular acidification. For three groups tested, the contribution of glycolysis represents about 90% of the total acidification observed (Fig. 4F). As shown in Fig. 4G and H, basal glycolysis in ectopic ESCs was 64% higher than eutopic ESCs ($P < 0.0001$) and 168% higher than controlled ESCs ($P < 0.0001$), compensatory glycolysis in ectopic ESCs was 21% higher than eutopic ESCs ($P < 0.001$) and 139% higher than controlled ESCs ($P < 0.0001$). These differences among three groups concurred with the glycolysis data measured by the glycolytic stress test kit (Fig. 4D). Furthermore, basal mitoOCR/glycoPER ratio was calculated and the ratio in ectopic ESCs were obviously decreased compared to eutopic ESCs ($P < 0.0001$) and controlled ESCs ($P < 0.0001$) (Fig. 4I).

3.4. SOD2 expression increased in ectopic ESCs

We investigate the functional relevance of superoxide dismutase-2 (SOD2) in endometriosis using immunochemistry. SOD2 immune expression was distributed strongly in the cytoplasm of the surface epithelial and stromal cells, especially stromal cells in the ectopic endometrium, and also in glandular epithelium cells and stromal cells of eutopic endometrium, while controlled endometrium showed low

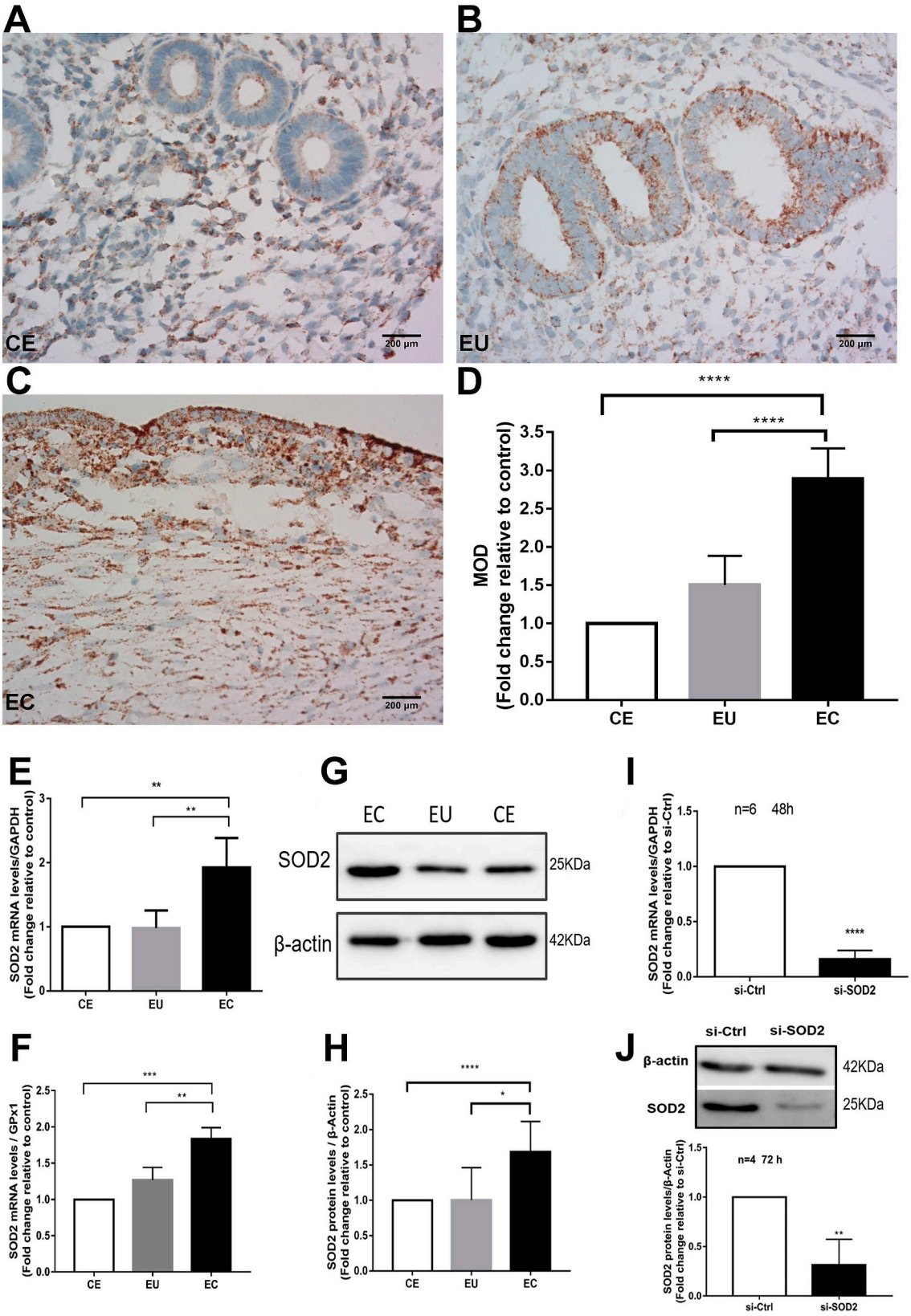

Fig. 5. SOD2 expression increased in ectopic endometrium and cells. A–C: Immunohistochemical staining for SOD2 in endometrium at proliferative phases. A. The controlled endometrium (CE), magnification, × 400. B. The eutopic endometrium (EU), magnification, × 400. C. The ectopic endometrium (EC), magnification, × 400. D. Statistical analysis indicated changes in SOD2 expression in ectopic endometrium, eutopic and controlled endometrium. E. Increased SOD2 mRNA expression was observed in ectopic ESCs (EC) compared with eutopic ESCs (EU) and controlled ESCs (CE). G–H: Increased SOD2 protein expression was observed in ectopic ESCs (EC) compared with eutopic ESCs (EU) and controlled ESCs (CE). F. The ratio SOD2/GPx1 in mRNA levels was significantly higher in ectopic ESCs compared to eutopic ESCs (**P < 0.01) and controlled ESCs (***P < 0.001). I–J: SOD2 mRNA and protein expression were reduced using siRNA transfection in ectopic ESCs.

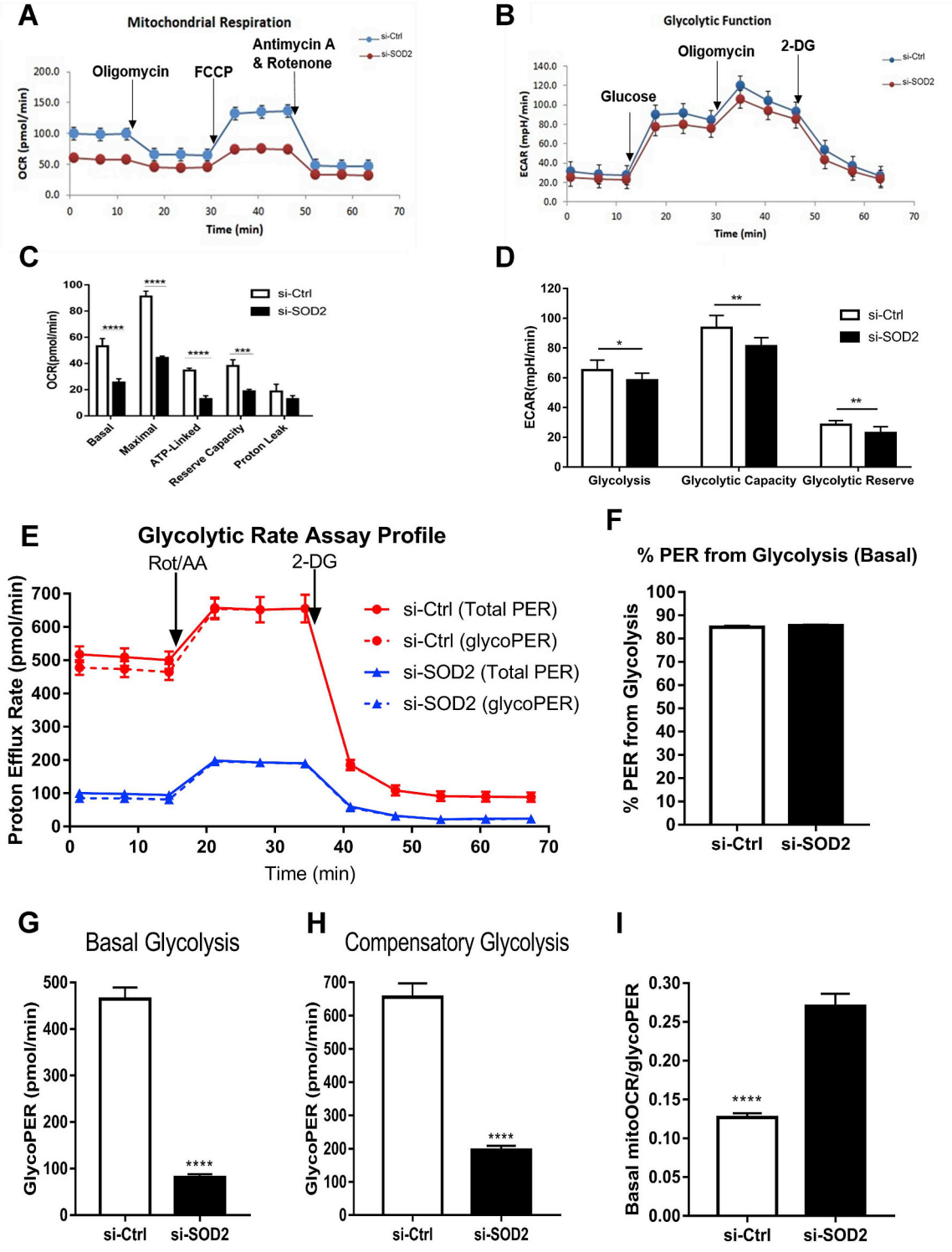

Fig. 6. SOD2 preserved ectopic ESCs mitochondrial respiration. A. Reduced SOD2 levels significantly decreased mitochondrial respiration in si-SOD2 transfected ectopic ESCs. B. Reduced SOD2 levels didn't increase glycolysis in si-SOD2 transfected ectopic ESCs. C. Basal OCR, maximal OCR, ATP-linked OCR and respiratory reserve capacity (max OCR - basal OCR) were significantly attenuated with si-RNA mediated SOD2 knockdown in ectopic ESCs. D. Glycolysis, glycolytic capacity and glycolytic reserve were slightly reduced with si-RNA mediated SOD2 knockdown in ectopic ESCs. E. Representative of glycolytic rate assay profile in two groups. F. The %PER from glycolysis of two groups. G. Reduced SOD2 levels significantly decreased basal glycolysis in si-SOD2 transfected ectopic ESCs. H. Reduced SOD2 levels significantly decreased compensatory glycolysis in si-SOD2 transfected ectopic ESCs. I. Basal mitoOCR/glycoPER ratio was calculated and the ratio was significantly higher in si-SOD2 transfected ectopic ESCs than the control.

expression of SOD2 (Fig. 5A–C). The SOD2 expression in endometrium included the SOD2 expression in endometrial epithelium and stromal cells. As shown in Fig. 5D, statistical analysis indicated that SOD2 expression in ectopic endometrium was higher than that in eutopic ($P < 0.0001$) and controlled endometrium ($P < 0.0001$). Due to high expression of SOD2 in endometrial stromal cells, we further conducted RT-qPCR and western blot in endometrial stromal cells. The SOD2 mRNA expression was significantly elevated in ectopic ESCs compared to eutopic ESCs ($P < 0.01$) and controlled ESCs ($P < 0.01$, Fig. 5E). As expected, the SOD2 protein also expressed higher in ectopic ESCs than eutopic ESCs ($P < 0.05$) and controlled ESCs ($P < 0.0001$, Fig. 5G and H). These results suggested that SOD2 was significantly upregulated in ectopic endometrium, especially ectopic ESCs. To confirm the antioxidant enzymes imbalance in ESCs, the ratio SOD2/GPx1 in mRNA levels were determined in three groups (Fig. 5F). The ratio was significantly elevated in ectopic ESCs compared to eutopic ESCs ($P < 0.01$) and controlled ESCs ($P < 0.001$).

3.5. SOD2 knockdown significantly inhibited mitochondrial respiration of ectopic ESCs

Due to SOD2 functioning in protecting mitochondria from excess $O_2^{\cdot-}$, we further examined the effect of SOD2 knockdown on mitochondrial respiration and the glycolytic rate by using extracellular flow analysis (Seahorse Biosciences). We performed siRNA-mediated knockdown of SOD2 in ectopic endometrial stromal cells. The results showed that SOD2 mRNA and protein levels significantly decreased detecting at 48 and 72 h after siRNA transfection, respectively ($P < 0.0001$, $P < 0.01$) (Fig. 5I and J). As shown in Fig. 6A and C, significant reduction of basal OCR, maximal OCR and ATP-linked OCR were observed in si-SOD2 treated cells compared with si-Ctrl treated cells ($P < 0.0001$, $P < 0.0001$, $P < 0.0001$, respectively). Furthermore, respiratory reserve capacity, representing the ability of cells to increase respiration as adaption to physiologic stress, was significantly reduced with inhibited SOD2 levels ($P < 0.001$). These results demonstrated that the si-SOD2 treated cells exhibited signs of damage and impaired mitochondrial respiration, implying that SOD2 makes an important impact in maintaining mitochondrial function. Compared to reduction in OCR, ECAR had slight reduction after knockdown of SOD2 (Fig. 6B). As shown in Fig. 6D, small reduction of glycolysis, glycolytic capacity and glycolytic reserve were observed in si-SOD2 treated cells compared with si-Ctrl treated cells ($P < 0.05$, $P < 0.01$, $P < 0.01$, respectively). We also used the Glycolytic Rate Assay to specifically study the effect of decreased SOD2 on glycolysis (Fig. 6E). For two groups tested, the contribution of glycolysis represents about 85% of the total acidification observed (Fig. 6F). Compared to the control, si-SOD2 group exhibited significant decreased basal glycolysis and compensatory glycolysis (Fig. 6G and H). We also calculated basal mitoOCR/glycoPER ratio, which was much lower in si-Ctrl treated cells than that in si-SOD2 treated cells ($P < 0.0001$) (Fig. 6I).

3.6. Reduced SOD2 attenuated proliferation and migration of ectopic ESCs

For further evaluation of the potential role of SOD2 in cell proliferation and migration, we performed CCK-8 counting assay and transwell migration assay after knockdown of SOD2 in ectopic ESCs. We found that OD was lower in si-SOD2 treated cells than si-Ctrl treated cells ($P < 0.001$), illustrating that reduced SOD2 significantly dampened cell proliferation (Fig. 7A). Besides, in Fig. 7B, the number of migrated cells in the si-SOD2 treated groups was significantly decreased compared with that in the si-Ctrl group, indicating that the migratory ability of ectopic ESCs were significantly attenuated after SOD2 inhibition ($P < 0.001$) (Fig. 7C).

3.7. Knockdown of SOD2 promoted loss of mitochondrial membrane potential in ectopic ESCs

The mitochondrial membrane potential (MMP, $\Delta\Psi m$) is a key indicator of mitochondrial function and cellular viability. Considering that SOD2 is protecting mitochondria from superoxide, we examined MMP of ectopic ESCs after si-RNA transfection to assess whether SOD2 knockdown would impair mitochondrial. The MMP was significantly decreased in si-SOD2 treated cells than control group ($P < 0.001$) (Fig. 7D). Hence, the experiment demonstrated that SOD2 inhibition impaired the function of mitochondria in the apoptotic pathway.

4. Discussion

Endometriosis is considered as a benign gynecological disease but shares some features with cancer, like invasion, proliferation and migration. Many studies indicate that oxidative stress positively associated with the proliferation and migration of endometrial cells in the peritoneal cavity, promoting endometriosis and infertility [4,5]. Mitochondria are a major source for ROS generation and ATP production, suggesting that mitochondria play a major role in the pathogenesis and development of endometriosis. However, little is known about mitochondrial changes of ectopic ESCs and how mitochondrial antioxidant enzyme SOD2 participates in the development of endometriosis. In the present study, we found active mitochondrial function with increased ROS generation in ovarian endometriosis. Also, we demonstrated that SOD2 was highly expressed in ectopic ESCs to deal with oxidative stress in endometriosis. Besides its antioxidant function, SOD2 also played a significant role in maintaining mitochondrial function and promoting proliferation and migration in ovarian endometriosis.

The endometrium is mainly consist of epithelium cells and stromal cells. The columnar epithelium is supported by a stromal cell foundation [34]. The ESCs affect epithelial function by producing growth factors and cytokines that work on epithelium cells. ESCs migrate to and survive in ectopic locations, forming the main characteristic of endometriosis [35], which urged us to pay emphasis study on ESCs.

During OXPHOS, some electrons escape from the chain and rapidly interact with oxygen molecule to form superoxide anion, the main ROS in mitochondria [36,37]. MtDNA damage will disturb the normal operation of mitochondrial respiratory chain and aggravate oxidative stress. No changes of mtDNA replication and transcription were found in ectopic ESCs in our study. We found mitochondrial superoxide increased significantly in ectopic ESCs, which elucidated oxidative stress in endometriosis. Alterations in mitochondrial structure, especially cristae will result in producing more ROS through influencing OXPHOS function. In 1971, Hackenbrock [38] revealed the relation between ultrastructure and energetic state. With low or high ADP concentrations for OXPHOS, mitochondria adopted orthodox or condensed conformation. Recent studies have found mitochondrial can change their morphology and remodel cristae in response to stress conditions [39]. For example, exposure to hypoxia or oxidative stress, mitochondria elongated [40]. Mitochondrial elongation is also considered to be an adaptation mechanism related with increased mitochondrial bioenergetic efficiency [39]. In our experiments, mitochondrial elongation had been found in ectopic ESCs. We suggest it is because mitochondria of ectopic ESCs stay in the long-term oxidative stress environment and they are forced to produce enough energy for the growth of ectopic lesions. In return, mitochondria of ectopic ESCs will generate more ROS through this process. Mitochondria remodel from class I-IV during apoptosis [25]. The ectopic ESCs showed some class II and III mitochondria, which are not efficient in OXPHOS, but ectopic ESCs can fulfill their energy demand by a compensatory increase in matrix density and mitochondrial numbers, as our results showed more mitochondria in ectopic ESCs. Mitochondria move along the cytoskeleton

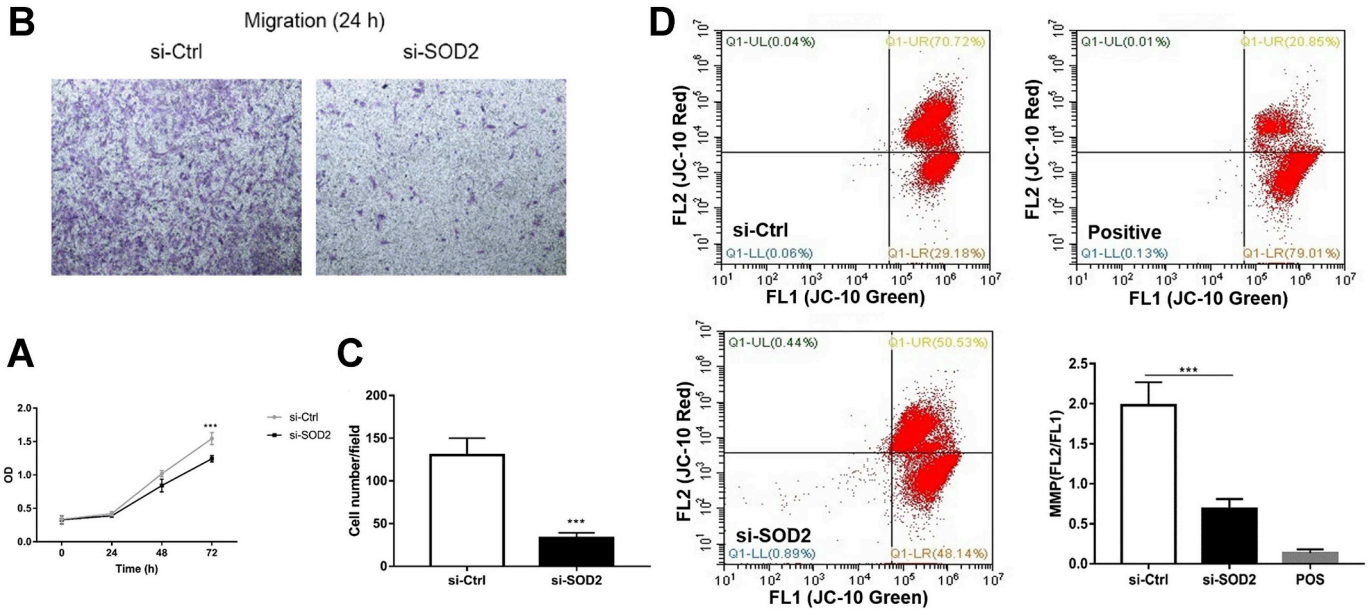

Fig. 7. Effects of si-SOD2 on ectopic ESCs proliferation, migration and apoptosis. A. Reduced SOD2 significantly attenuated proliferation in si-SOD2 transfected ectopic ESCs. B, C: Reduced SOD2 attenuated migration in si-SOD2 transfected ectopic ESCs. D. Effects of si-SOD2 on mitochondria-mediated apoptosis in ectopic ESCs. Loss of mitochondrial membrane potential (MMP) in si-SOD2 transfected ectopic ESCs was estimated by flow cytometry. Cells forming JC-10 aggregates are in the upper right quadrant and the JC-10 monomer is in the lower right quadrant. The relative signal intensities of JC-10 aggregates were normalized to JC-10 monomers. For a positive control, cells were incubated with FCCP under the same culture conditions.

to actively functional areas in cells and cytoskeleton play important roles in migration. In general, the more mitochondria, the more metabolic activity and cell migration. Mitochondria in ectopic ESCs expended cristae area and become longer in shape, thus providing more places for metabolic bioenergetics, intracellular biological oxidation and ROS output. As for mitochondrial function, significant increases in OCR and ECAR were observed in ectopic ESCs. This increased energy demand causes more stress on the mitochondrial respiration chain, and may contribute to enhance ROS [41]. Furthermore, basal mitoOCR/glycoPER ratio was lower than 1, indicting cellular adaptation towards glycolytic metabolism in three groups and the presence and role of hypoxia in the endometrium [42]. We found that hypoxia is more severe in ectopic ESCs. According to Sampson's theory, one of the main theories about endometriosis, retrograde menstruation carry apoptotic endometrial tissues into ectopic lesions, with low blood supply and hypoxic stress. It is necessary to switch from mitochondrial OXPHOS to glycolysis in order to survive in the hypoxic microenvironment. Mitochondrial structure is related to oxygen partial pressure, energy demand, and mitochondrial respiration. Mitochondrial structural changes in ectopic ESCs could be a response to hypoxic environment, which may be more efficient in glycolysis, thus facilitating survival of ectopic endometrial cells. The ratio of ectopic ESCs was less than other two groups, indicating that ectopic ESCs depend more on glycolysis to meet bioenergetic and biosynthetic demands. Extensive glycolysis overproduces lactate, which increase cell migration and invasion, angiogenesis, all of which are crucial in the development of endometriosis [43]. Recent studies have shown high levels of lactate and glycolysis markers in the peritoneal fluid of women with endometriosis [44]. With efficient energy supply and increased lactate production, ectopic ESCs proliferate and migrate in the ovary, gradually forming ectopic lesions. This process also stimulates local inflammatory response and fibrosis, thus aggravating ovarian damage.

Under oxidative stress, cells regulate various adaptation mechanisms to eliminate ROS. Oxidative stress-induced SOD2 expression is considered as an important cellular adaption mechanism [45]. Regardless of the menstrual cycle in patients with endometriosis, SOD was persistently overexpressed [21]. In our study, we found increased RNA and protein expression of SOD2 in ectopic ESCs, especially cytoplasm of stromal cells. Considering that ectopic ESCs generated more ROS and endometriosis cells were under sustained ROS stress, SOD2 overexpression were of limited capacity in reducing this stress. We may presume that ectopic ESCs may exhaust ROS-buffering capacity after heavily utilizing adaptation mechanisms, thus tending to be more sensitive to oxidative damage. Furthermore, reduced SOD2 significantly decreased the mitochondrial oxidative phosphorylation and glycolysis, implying that SOD2 also maintained mitochondrial respiration function. In our study, reduced SOD2 also inhibited cell proliferation and migration, through its reduced mitochondrial function. Some studies have found that SOD2 overexpression enhances invasiveness and migration by different mechanisms [46,47]. Under normal physiological conditions, the ratio $O_2^{\cdot-}/H_2O_2$ are well within the mitochondrial buffering capacity. However, when SOD2 levels increase, the mitochondrial glutathione buffering capacity may be overwhelmed by H_2O_2. Researchers revealed that SOD2-induced H_2O_2 increase led to ERK1/2 activation and subsequent increases in matrix metalloproteinases, which strongly associated with enhanced metastasis [48–50]. Further, migration and invasion of the SOD2 overexpressed cells was inhibited following overexpression of catalase, indicating that the migratory/invasive phenotype is H_2O_2 dependent [46]. We found the ratio SOD2/GPx1 in ESCs was highest in ectopic ESCs among three groups, thus we may speculate that high levels of H_2O_2 in mitochondria of ectopic ESCs. However, in this study, we didn't study on the specific relationship between H_2O_2 and endometriosis.

The permeability of mitochondrial outer membrane is a key step in the development of apoptosis. This process involves changing the permeability of mitochondrial membrane by opening the permeability transition pore (PTP), thereby decreasing the mitochondrial membrane potential, apoptotic factors such as cytochrome c releasing from the mitochondria to the cytoplasm, causing mitochondria-mediated apoptosis. Decreased mitochondrial membrane potential is a hallmark of early apoptosis [51,52]. We evaluated the function of mitochondria in the apoptosis using the mitochondrial membrane potential (MMP) assay. In our study, attenuated SOD2 expression lowered MMP of ectopic ESCs, indicating that SOD2 knockdown induced apoptosis

through decreasing mitochondrial membrane potential and increasing ROS production in endometriotic cells. SOD2 has a protective role for mitochondria against oxidative stress and apoptosis, which benefit ectopic ESCs growth and migration. ROS play an important role in regulating myriad cellular processes, including apoptosis and immune response [53]. Here the anti-apoptotic role of SOD2 has primarily been attributed to its antioxidant activity. Studies have shown that SOD2 protects cells from radiotherapy induced apoptosis for it stabilizes the mitochondrial membrane and leads to decreased caspase3 activation when treated with ionizing radiation [54]. Mitochondria-mediated apoptosis has some important marker proteins like Bax, Cytc and caspase, questions remain regarding the effectiveness of overexpressed SOD2 on these proteins in endometriosis.

In conclusion, we identified overexpressed SOD2 coupled to preserved mitochondrial functions but increased mitochondrial superoxide production in endometriosis. It represents oxidative stress in endometriosis has exhausted antioxidant mechanisms of the body. Thus, mitochondrial superoxide scavenging can be proposed as a therapeutic option to prevent the development of ovarian endometriosis. MitoTEMPO, which specifically scavenge mitochondrial superoxide, has been reported to prevent metastasis in human tumor models [55]. It may serve as a promising antioxidant in endometriosis treatment.

Conflicts of interest

The authors declare no conflicts of interest.

Acknowledgements

This work was supported by the National Natural Science Foundation of China (No. 81170547), Natural Science Foundation of Zhejiang Province (LY18H040004) and Research Funding of National Health Commission (WKJ-ZJ-1907).

References

[1] R. Garry, Is insulin resistance an essential component of PCOS?: the endometriosis syndromes: a clinical classification in the presence of aetiological confusion and therapeutic anarchy, Hum. Reprod. 19 (4) (2004) 760–768.
[2] V.M. Rice, Conventional medical therapies for endometriosis, Ann. N. Y. Acad. Sci. 955 (2002) 343–352 discussion 389-93, 396-406.
[3] P.A. Klemmt, et al., Endometrial cells from women with endometriosis have increased adhesion and proliferative capacity in response to extracellular matrix components: towards a mechanistic model for endometriosis progression, Hum. Reprod. 22 (12) (2007) 3139–3147.
[4] A. Van Langendonckt, F. Casanas-Roux, J. Donnez, Oxidative stress and peritoneal endometriosis, Fertil. Steril. 77 (5) (2002) 861–870.
[5] C. Ngo, et al., Reactive oxygen species controls endometriosis progression, Am. J. Pathol. 175 (1) (2009) 225–234.
[6] S.H. Kao, et al., Oxidative damage and mitochondrial DNA mutations with endometriosis, Ann. N. Y. Acad. Sci. 1042 (2005) 186–194.
[7] R. Nunez-Calonge, et al., Oxidative stress in follicular fluid of young women with low response compared with fertile oocyte donors, Reprod. Biomed. Online 32 (4) (2016) 446–456.
[8] P. Santulli, et al., Protein oxidative stress markers in peritoneal fluids of women with deep infiltrating endometriosis are increased, Hum. Reprod. 30 (1) (2015) 49–60.
[9] E. Turkyilmaz, et al., Evaluation of oxidative stress markers and intra-extracellular antioxidant activities in patients with endometriosis, Eur. J. Obstet. Gynecol. Reprod. Biol. 199 (2016) 164–168.
[10] J.C. Rosa e Silva, et al., Serum markers of oxidative stress and endometriosis, Clin. Exp. Obstet. Gynecol. 41 (4) (2014) 371–374.
[11] A. Harlev, S. Gupta, A. Agarwal, Targeting oxidative stress to treat endometriosis, Expert Opin. Ther. Targets 19 (11) (2015) 1447–1464.
[12] A. Andrisani, et al., Increased oxidation-related glutathionylation and carbonic anhydrase activity in endometriosis, Reprod. Biomed. Online 28 (6) (2014) 773–779.
[13] M. Nagata, Inflammatory cells and oxygen radicals, Curr. Drug Targets - Inflamm. Allergy 4 (4) (2005) 503–504.
[14] J. Donnez, et al., Oxidative stress in the pelvic cavity and its role in the pathogenesis of endometriosis, Fertil. Steril. 106 (5) (2016) 1011–1017.
[15] B.D. McKinnon, et al., Kinase signalling pathways in endometriosis: potential targets for non-hormonal therapeutics, Hum. Reprod. Update 22 (3) (2016) 382–403.
[16] A. Chatterjee, E. Mambo, D. Sidransky, Mitochondrial DNA mutations in human cancer, Oncogene 25 (34) (2006) 4663–4674.
[17] S. Cho, et al., Mitochondria DNA polymorphisms are associated with susceptibility to endometriosis, DNA Cell Biol. 31 (3) (2012) 317–322.
[18] S. Govatati, et al., Mitochondrial displacement loop alterations are associated with endometriosis, Fertil. Steril. 99 (7) (2013) 1980-6.e9.
[19] A. Miar, et al., Manganese superoxide dismutase (SOD2/MnSOD)/catalase and SOD2/GPx1 ratios as biomarkers for tumor progression and metastasis in prostate, colon, and lung cancer, Free Radic. Biol. Med. 85 (2015) 45–55.
[20] H. Ota, et al., Endometriosis and free radicals, Gynecol. Obstet. Investig. 48 (Suppl 1) (1999) 29–35.
[21] H. Ota, et al., Immunohistochemical assessment of superoxide dismutase expression in the endometrium in endometriosis and adenomyosis, Fertil. Steril. 72 (1) (1999) 129–134.
[22] H. Ota, et al., Aberrant expression of glutathione peroxidase in eutopic and ectopic endometrium in endometriosis and adenomyosis, Fertil. Steril. 74 (2) (2000) 313–318.
[23] L.P. Hemachandra, et al., Mitochondrial superoxide dismutase has a protumorigenic role in ovarian clear cell carcinoma, Cancer Res. 75 (22) (2015) 4973–4984.
[24] J.P. Piret, et al., Differential toxicity of copper (II) oxide nanoparticles of similar hydrodynamic diameter on human differentiated intestinal Caco-2 cell monolayers is correlated in part to copper release and shape, Nanotoxicology 6 (7) (2012) 789–803.
[25] L. Scorrano, et al., A distinct pathway remodels mitochondrial cristae and mobilizes cytochrome c during apoptosis, Dev. Cell 2 (1) (2002) 55–67.
[26] B.P. Dranka, et al., Assessing bioenergetic function in response to oxidative stress by metabolic profiling, Free Radic. Biol. Med. 51 (9) (2011) 1621–1635.
[27] L. Schneider, et al., Differentiation of SH-SY5Y cells to a neuronal phenotype changes cellular bioenergetics and the response to oxidative stress, Free Radic. Biol. Med. 51 (11) (2011) 2007–2017.
[28] A.A. Gerencser, et al., Quantitative microplate-based respirometry with correction for oxygen diffusion, Anal. Chem. 81 (16) (2009) 6868–6878.
[29] S.A. Mookerjee, et al., The contributions of respiration and glycolysis to extracellular acid production, Biochim. Biophys. Acta 1847 (2) (2015) 171–181.
[30] S.A. Mookerjee, M.D. Brand, Measurement and analysis of extracellular acid production to determine glycolytic rate, JoVE (106) (2015) e53464.
[31] S.A. Mookerjee, et al., Quantifying intracellular rates of glycolytic and oxidative ATP production and consumption using extracellular flux measurements, J. Biol. Chem. 292 (17) (2017) 7189–7207.
[32] R. Demir, et al., Structural differentiation of human uterine luminal and glandular epithelium during early pregnancy: an ultrastructural and immunohistochemical study, Placenta 23 (8–9) (2002) 672–684.
[33] F.J. Miller, et al., Precise determination of mitochondrial DNA copy number in human skeletal and cardiac muscle by a PCR-based assay: lack of change of copy number with age, Nucleic Acids Res. 31 (11) (2003) e61.
[34] H. Zhou, et al., Exendin-4 enhances the migration of adipose-derived stem cells to neonatal rat ventricular cardiomyocyte-derived conditioned medium via the phosphoinositide 3-kinase/Akt-stromal cell-derived factor-1alpha/CXC chemokine receptor 4 pathway, Mol. Med. Rep. 11 (6) (2015) 4063–4072.
[35] Q. Zhao, et al., Effect of Mst1 on endometriosis apoptosis and migration: role of Drp1-related mitochondrial fission and parkin-required mitophagy, Cell. Physiol. Biochem. 45 (3) (2018) 1172–1190.
[36] H. Saybasili, et al., Effect of mitochondrial electron transport chain inhibitors on superoxide radical generation in rat hippocampal and striatal slices, Antioxidants Redox Signal. 3 (6) (2001) 1099–1104.
[37] K. Staniek, et al., Mitochondrial superoxide radical formation is controlled by electron bifurcation to the high and low potential pathways, Free Radic. Res. 36 (4) (2002) 381–387.
[38] C.R. Hackenbrock, et al., Oxidative phosphorylation and ultrastructural transformation in mitochondria in the intact ascites tumor cell, J. Cell Biol. 51 (1) (1971) 123–137.
[39] S. Cogliati, J.A. Enriquez, L. Scorrano, Mitochondrial cristae: where beauty meets functionality, Trends Biochem. Sci. 41 (3) (2016) 261–273.
[40] M. Jendrach, et al., Short- and long-term alterations of mitochondrial morphology, dynamics and mtDNA after transient oxidative stress, Mitochondrion 8 (4) (2008) 293–304.
[41] H. Pelicano, D. Carney, P. Huang, ROS stress in cancer cells and therapeutic implications, Drug Resist. Updates 7 (2) (2004) 97–110.
[42] J.A. Maybin, A.A. Murray, P.T.K. Saunders, Hypoxia and hypoxia inducible factor-1alpha are required for normal endometrial repair during menstruation, 9 (1) (2018) 295.
[43] F. Hirschhaeuser, U.G. Sattler, W. Mueller-Klieser, Lactate: a metabolic key player in cancer, Cancer Res. 71 (22) (2011) 6921–6925.
[44] V.J. Young, et al., Transforming growth factor-beta induced Warburg-like metabolic reprogramming may underpin the development of peritoneal endometriosis, J. Clin. Endocrinol. Metab. 99 (9) (2014) 3450–3459.
[45] Y. Chen, et al., Tumour suppressor SIRT3 deacetylates and activates manganese superoxide dismutase to scavenge ROS, EMBO Rep. 12 (6) (2011) 534–541.
[46] K.M. Connor, et al., Manganese superoxide dismutase enhances the invasive and migratory activity of tumor cells, Cancer Res. 67 (21) (2007) 10260–10267.
[47] N. Hempel, P.M. Carrico, J.A. Melendez, Manganese superoxide dismutase (Sod2) and redox-control of signaling events that drive metastasis, Anti Cancer Agents Med. Chem. 11 (2) (2011) 191–201.
[48] A.C. Ranganathan, et al., Manganese superoxide dismutase signals matrix metalloproteinase expression via H2O2-dependent ERK1/2 activation, J. Biol. Chem. 276 (17) (2001) 14264–14270.
[49] P.R. Nagareddy, et al., Maintenance of adrenergic vascular tone by MMP transactivation of the EGFR requires PI3K and mitochondrial ATP synthesis, Cardiovasc.

Res. 84 (3) (2009) 368–377.
[50] K.K. Nelson, et al., Elevated sod2 activity augments matrix metalloproteinase expression: evidence for the involvement of endogenous hydrogen peroxide in regulating metastasis, Clin. Cancer Res. 9 (1) (2003) 424–432.
[51] V. Gogvadze, S. Orrenius, B. Zhivotovsky, Multiple pathways of cytochrome c release from mitochondria in apoptosis, Biochim. Biophys. Acta 1757 (5–6) (2006) 639–647.
[52] A.M. Abdel-Latif, H.A. Abuel-Ela, S.H. El-Shourbagy, Increased caspase-3 and altered expression of apoptosis-associated proteins, Bcl-2 and Bax in lichen planus, Clin. Exp. Dermatol. 34 (3) (2009) 390–395.
[53] J.M. Gutteridge, B. Halliwell, Comments on review of free radicals in biology and medicine, second ed., by Barry Halliwell and John M. C. Gutteridge, Free Radic Biol Med vol. 12, (1) (1992) 93–95.
[54] M.W. Epperly, et al., Manganese superoxide dismutase (SOD2) inhibits radiation-induced apoptosis by stabilization of the mitochondrial membrane, Radiat. Res. 157 (5) (2002) 568–577.
[55] P.E. Porporato, et al., A mitochondrial switch promotes tumor metastasis, Cell Rep. 8 (3) (2014) 754–766.